Jurnal Arus Elektro Indonesia (JAEI) Vol. 10, No. 1, Maret 2024
ISSN. 2502-3608; e-ISSN. 2443-2318, Terakreditasi Sinta 5
DOI: 10.19184/jaei.v10i1.39120

# Testing and Comparison of SN754410N and L293D Driver IC Variants

Victor Phoa[1], and Hariyono Rakhmad[2]
Department of Information Technology, Politeknik Negeri Jember
Jl. Mastrip Kotak Pos 164, Jember, Jawa Timur, Indonesia 68101
victor@polije.ac.id[1], hariyono_r@polije.ac.id[2]

**Abstrak**

**IC *driver* berbasis transistor populer yakni L293D telah diproduksi oleh beberapa pabrikan berbeda dan ada pula yang memiliki peningkatan fungsi seperti pada IC SN754410N. Namun penggantian IC *driver* dari pabrikan yang sama ataupun berbeda kadang ditemukan adanya masalah kompatibilitas seperti tidak responsifnya *driver* dalam mengendalikan motor. Untuk mengetahui alasan detil komprehensif yang menyebabkan masalah tersebut, maka pada dalam penelitian ini menguji kemampuan penghantaran arus dan tundaan penyaklaran untuk IC dari fabrikasi ST, HLF, dan SN754410N. Dari hasil pengujian, ditemukan bahwa terdapat perbedaan kemampuan dalam penghantaran arus, perbedaan durasi tundaan penyaklaran, dan ditemukan pula IC yang mengalami kerusakan sebanyak 10 persen dari sampel dari fabrikasi ST.**

***Kata Kunci* — *Motor driver*, L293D, SN754410N.**

***Abstract***

***The popular transistor-based driver L293D has been produced by several different manufacturers and some have increased functions such as the SN754410N IC. However, replacing driver ICs from the same or different manufacturers sometimes found compatibility problems such as driver unresponsiveness in controlling the motor. To find out the comprehensive detail reasons that cause this problem, this study tested the current-carrying ability and switching delay for ICs from ST, HLF, and SN754410N fabrications. From the test results, it was found that there were differences in the ability to conduct current, and differences in the duration of the switching delay, and it was also found that the IC was damaged as much as 10 percent of the samples from the ST fabrication.***

***Keywords* — *Motor driver, L293D, SN754410N*.**

## I. Introduction

A motor driver IC is an integrated circuit device utilized as a motor controller or actuator in robots, toys, and various equipment with embedded systems [1] [2]. One of the most popular and cost-effective motor driver ICs is the L293D, which incorporates 4 Half-H drivers capable of controlling 2 DC motors in two rotation directions, functioning as 2 bridge drivers. This IC is manufactured by various electronic component producers. An enhanced replacement IC with the code SN754410N is also available, capable of controlling loads up to 1A, whereas the L293D IC itself is designed to handle loads up to 0.6A [3]. Despite the prevalence of MOSFET drivers, bipolar transistor drivers remain useful in many applications due to their simplicity, wide range of operation voltage, resilience against damage from voltage spikes and other transient events, and the fact that they do not require a charge pump, unlike MOSFET drivers [4] [5] [6].

In the general market, the most common L293D IC is the one with the manufacturing code marked ST (hereinafter referred to as ST), followed by the variant HLF (hereinafter referred to as HLF). The SN754410N itself was found without a manufacturing code (hereinafter referred to as SN754410N). For the HLF variant, there is no official datasheet from the manufacturer (Shenzhen Honglifa Electronics) and several sales sites refer to the L293D datasheet from TI (Texas Instruments) [7] and ST (STMicroelectronics) [8]. The latter appears to have entered the integrated circuit production scene around 2010, with a particular focus on IC replacements. However, there have been no reviews yet regarding the compatibility and quality of their L293D IC.

In various online forums, a number of users of the LD293D IC have expressed concerns about the quality of these components [9]. Instances have been reported where purchased ICs were found to be damaged or malfunctioning. Furthermore, debates surround the compatibility of this IC with its replacement, the SN754410. An issue discovered during the replacement of the ST IC with another variant resulted in the motor failing to operate. The prevalence of such problems raises questions: are the numerous ICs circulating in the market counterfeit, or do they reflect shortcomings in the production quality control process? Determining which aspect holds true poses a challenge. Although issues like these are frequently encountered, comprehensive studies to address them remain limited.

## II. Aim and Scope

Addressing existing issues, the authors undertook a study to compare the L293D variants with manufacturing codes ST and HLF, along with SN754410 (refer to Fig. 1). For this investigation, all three ICs were procured from an online

marketplace, each consisting of 20 component variants. ICs marked with ST and SN754410 were packaged in batch tubes, while those marked HLF came in a plastic clip pack. Subsequent tests were conducted to evaluate the delay time characteristics and the output delivery capability at a working voltage of 5V for each IC, using the same treatment with the ATmega328P microcontroller.

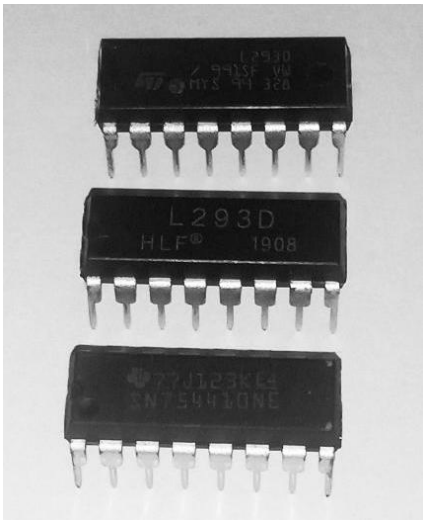


Fig. 1 3 variants of the ICs being compared

## III. Research Methods

The method employed in this test involves measuring virtual resistance both when the output is LOW and HIGH under a load. A smaller virtual resistance is considered indicative of better current-carrying ability. In the second test to determine the switching delay, the cycles required to switch from LOW to HIGH and vice versa from HIGH to LOW were counted. Fewer cycles required are indicative of more responsive output changes.

To carry out the test, a driver circuit (*H*) is connected through the circuit as shown in Fig. 2. The test is carried out with the Atmega328P microcontroller running at 18.432MHz clock. For each driver, Input *A* is connected to the digital output from the microcontroller (*PD3*) which is serialized with resistor *R1* to the input of the driver. *EN* is connected to the digital output (*PD4*) which is serialized with resistor *R2* to the enable of the driver. The *Y* section is connected to the microcontroller input which has digital input capability and ADC (*PC1*).

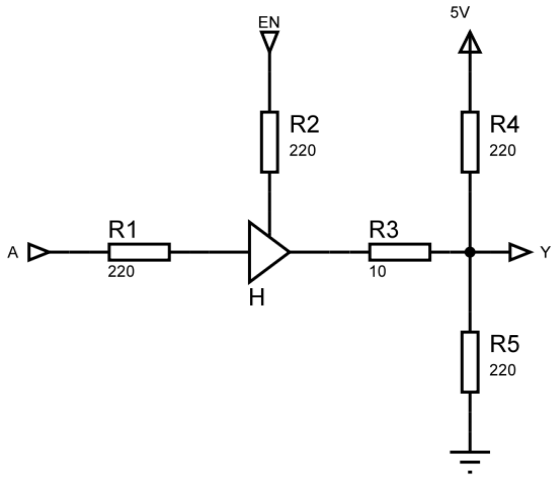


Fig. 2 The circuit schematic used in driver testing

In testing the output delivery capability, the microcontroller is in charge of activating the driver via *EN* and then testing the value of the *ADC* at *A* for high and low logic. High impedance when EN is LOW is also measured for reference. The code for testing the conductance of the output can be seen in Fig. 3. The virtual resistance value for a HIGH output ($R_{VH}$) at a working voltage of 5V can be calculated using formula (1), while the virtual resistance value for a LOW output ($R_{VL}$) can be determined using formula (2).

$$R_{VH} = \frac{\frac{15ADC}{64} - 230}{-\frac{ADC}{512} + 1} \quad (1)$$

$$R_{VL} = \frac{\frac{15ADC}{64} - 10}{-\frac{ADC}{512} + 1} \quad (2)$$

Code for measuring ADC values

```
//high impedance
digitalWrite(EN_PIN, LOW);
delay(2);
analogHighImpedance = analogRead(Y_PIN);
//LOW
digitalWrite(EN_PIN, HIGH);
digitalWrite(A_PIN, LOW);
delay(2);
analogEnableAndLowY = analogRead(Y_PIN);
//HIGH
digitalWrite(A_PIN, HIGH);
delay(2);
analogEnableAndHighY = analogRead(Y_PIN);
```

Fig. 3 Code for measuring the ADC value when the output at high impedance, HIGH, and LOW

ISSN. 2502-3608; e-ISSN. 2443-2318, Terakreditasi Sinta 5
DOI: 10.19184/jaei.v10i1.39120

The next task of the microcontroller is to test the switching delay. For this, the MCU instruction cycle count is used. For the delay test for high output, the enumeration is carried out after input *A* is set high until *Y* is detected as high by the MCU. For the delay test for low output, the enumeration is carried out after input *A* is set low until *Y* is detected low by the MCU. At this stage, *EN* is always set to high to keep the driver active.

Delay counter code for LOW to HIGH

```
#define NOP_1X asm volatile ("nop\n\t");
#define NOP_2X asm volatile ("nop\n\t");asm
volatile ("nop\n\t");
#define NOP_3X …
 …
#define NOP_25X …

uint8_t getLowToHighCycleCount(uint8_t
portdMask, uint8_t pincMask){
  bool b = false;
  dFlag = _BV(portdMask);
  cFlag = _BV(pincMask);
  for (uint8_t i=0; i<=25; i++){
    PORTD &= ~dFlag; //turn off first
    delayMicroseconds(4);
    cli();
    NOP_10X;//delay a bit
    switch(i){
      case 0:{
        NOP_1X;
        PORTD |= dFlag;
        value = PINC;
      }
      break;
      case 1:{
        NOP_1X;
        PORTD |= dFlag;
        NOP_1X;
        value = PINC;
      }
      break;
      case …:{
        …
      }
      break;
      case 25:{
        NOP_1X;
        PORTD &= dFlag; //turn off
        NOP_25X;
        value = PINC;
      }
      break;
    }
    sei();
    b = (value & cFlag) == 0;
    if (b) return i;
  }
  return 255; //out of reach
}
```

Fig. 4 Code section to count the delay from LOW to HIGH based on NOP cycles

To perform cycle counting, the instruction used is NOP which will be processed for 1 cycle by the MCU [10] [11]. By using the 18.432MHz clock, it is assumed that each cycle is 54.25 nanoseconds. This test is incremental in that the MCU is instructed to try to detect a change in *Y* from 0 to 25 NOP instruction cycles. The *getLowToHighCycleCount* function code abstraction used to count delays from LOW to HIGH can be seen in Fig. 4, and the *getHighToLowCycleCount* function used to count delays from HIGH to LOW can be seen in Fig. 5.

delay counter code for HIGH to LOW

```
uint8_t getHighToLowCycleCount(uint8_t
portdMask, uint8_t pincMask){
  bool b = false;
  dFlag = ~_BV(portdMask);
  cFlag = _BV(pincMask);
  for (uint8_t i=0; i<=25; i++){
    PORTD |= _BV(portdMask); //turn on
    delayMicroseconds(4);
    cli();
    NOP_10X;//delay a bit
    switch(i){
      case 0:{
        NOP_1X;
        PORTD &= dFlag; //turn off
        value = PINC;
      }
      break;
      case 1:{
        NOP_1X;
        PORTD &= dFlag; //turn off
        NOP_1X;
        value = PINC;
      }
      break;
      case …:{
        …
      }
      case 25:{
        NOP_1X;
        PORTD &= dFlag; //turn off
        NOP_25X;
        value = PINC;
      }
      break;
    }
    sei();
    b = (value & cFlag) == 0;
    if (b) return i;
  }

  return 255; //out of reach

}
```

Fig. 5 Code section to count the delay from HIGH to LOW based on NOP cycles

## IV. Results and Discussion

In the conducted tests, 2 out of the ST ICs were found to be defective, constituting 10 percent of the sample. These defects

include improper current immersion in response to both LOW and HIGH logic, along with unreasonable output delays in HIGH to LOW cycles. In contrast, no defects or malfunctions were identified in the samples of the other two IC types (HLF and SN754410N). These findings suggest a potential issue with the quality control of ST, highlighting the presence of defective ICs even when purchased in new packaging tubes. Detailed test results, including statistics for low outputs virtual resistance ($R_{VL}$), high outputs virtual resistance ($R_{VH}$), low to high cycle trip ($C_{TH}$), and high to low cycle trip ($C_{TL}$), are provided in Table 1.

TABLE I
VIRTUAL RESISTANCE TEST AND TRIP CYCLES RESULTS

| Test | | L293D (ST) | L293D (HLF) | SN 754410N |
|---|---|---|---|---|
| low logic virtual resistance (ohms) | defective highest | 323.465 | n/a | n/a |
| | typical highest | 43.721 | 43.246 | 42.775 |
| | typical average | 42.567 | 42.822 | 41.983 |
| | typical lowest | 42.305 | 42.775 | 41.839 |
| high logic virtual resistance (ohms) | defective highest | 65.875 | n/a | n/a |
| | typical highest | 46.136 | 47.122 | 46.136 |
| | typical average | 45.010 | 46.776 | 45.723 |
| | typical lowest | 44.198 | 46.136 | 45.161 |
| low to high cycle trip | defective highest | n/a | n/a | n/a |
| | typical highest | 13 | 10 | 12 |
| | typical average | 12.4 | 8.4 | 10.769 |
| | typical lowest | 11 | 7 | 9 |
| high to low cycle trip | defective highest | 10 | n/a | n/a |
| | typical highest | 4 | 5 | 6 |
| | typical average | 3.105 | 4.4 | 4.769 |
| | typical lowest | 3 | 3 | 4 |

While assessing the current-carrying capabilities in relation to its virtual resistance (refer to Fig. 6-9), distinct differences were observed in the performance of current sinking indication between LOW and HIGH outputs for all variants. The SN754410N excels in sinking average current for the LOW output, followed by the ST variant, and the HLF variant lags behind. Despite being the least efficient in current delivery, the HLF demonstrates the narrowest range of resistance variation, followed by SN754410N, and lastly ST. Notably, in the defective ST variant, the ability to conduct current at LOW logic was significantly diminished.

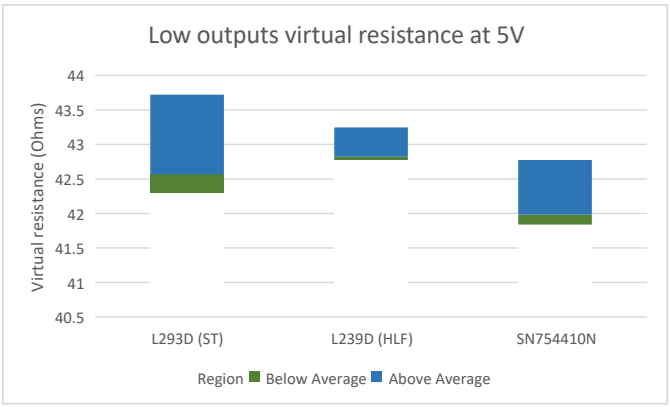


Fig. 6 Low outputs' virtual resistance region, where SN54410N has the lowest resistance, is followed by the ST variant, and the HLF variant lags behind. Despite being the least, the HLF demonstrates the narrowest range of resistance variation.

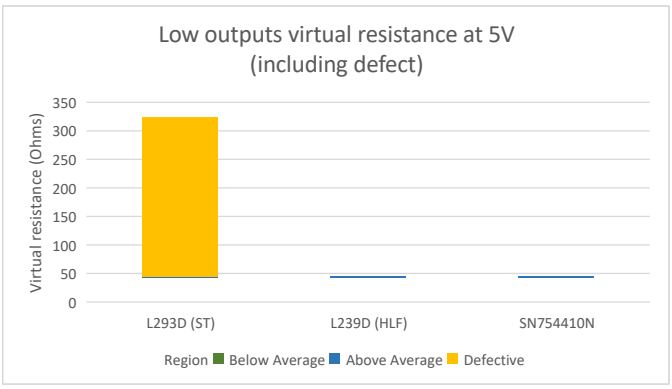


Fig. 7 Low outputs' virtual resistance region, including the defective ICs of L293D (ST) compared to L293D (HLF) and SN754410N, shows an increase in resistance, indicating that the ability of the ST variant to conduct current was significantly diminished.

In the HIGH output test, ST demonstrates the most effective capability to deliver average current conduction, followed by SN754410N, while HLF exhibits the lowest performance. While the resistance variation range of ST is larger than the other two variants, its upper limit matches that of the SN754410N IC. However, the average virtual resistance is consistently higher than the LOW output sinking for all IC variants. In the case of the defective ST IC, there is a reduction in the ability to conduct current at HIGH logic.

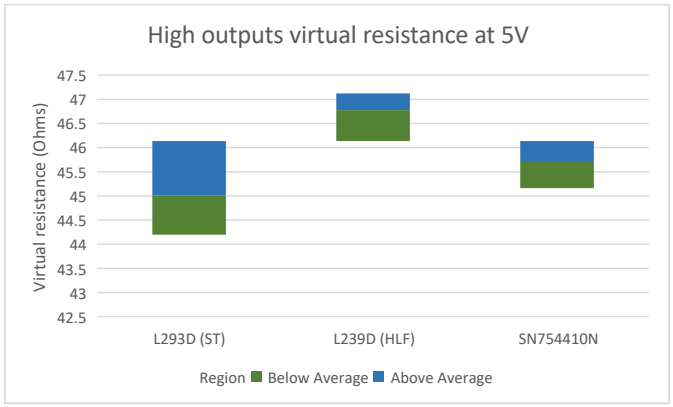


Fig. 8 High outputs' virtual resistance region indicates that ST ICs have the most effective capability in average current conduction, followed by SN754410N, with HLF exhibiting the lowest performance

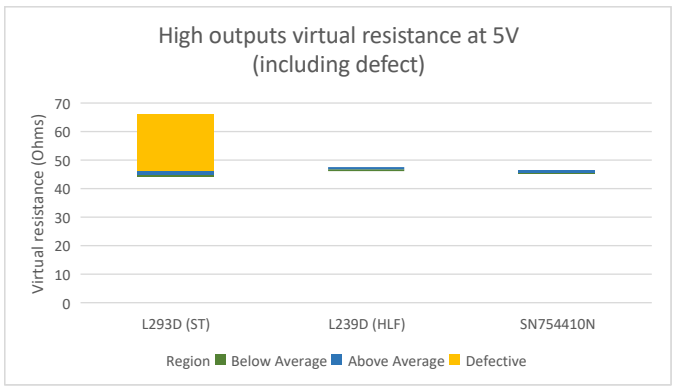


Fig. 9 In the high outputs' virtual resistance region, including the defective ICs of L293D (ST) compared to L293D (HLF) and SN754410N, there is an increase in resistance, indicating a reduced capability to conduct current when defective

When testing the switching delay from LOW to HIGH (refer to Fig. 10), the HLF IC exhibits the most favorable average response to switching, followed by SN754410N, and lastly ST. Despite having the longest switching delay, the range of delay variations for ST is minimal. Notably, in this test, the presence of a defective IC did not have an observable effect on the delay.

During testing of the switching delay from HIGH to LOW (refer to Fig. 11-12), the ST IC exhibited the most favorable average response to switching with the smallest range of delay variations. The HLF IC took the second position, followed by SN754410N. It was observed that the switching delay from HIGH to LOW states for all IC variants is faster than that from LOW to HIGH states. Notably, the testing revealed an impact of the defective IC on the delay length, particularly in the case of the ST IC, where the delay time became longer.

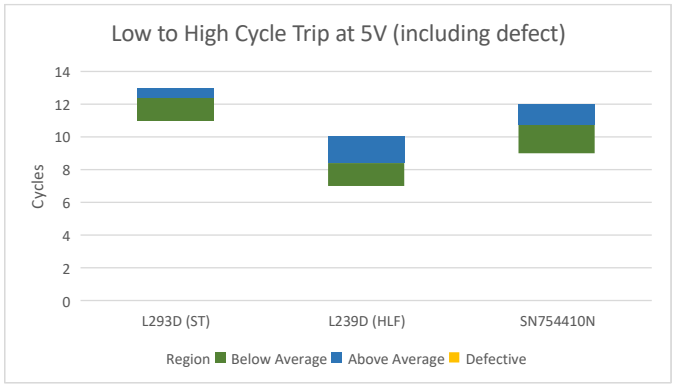


Fig. 10 Low to High cycle trip region of L293D (ST), L293D (HLF), and SN754410N (note that defects do not affect the test results)

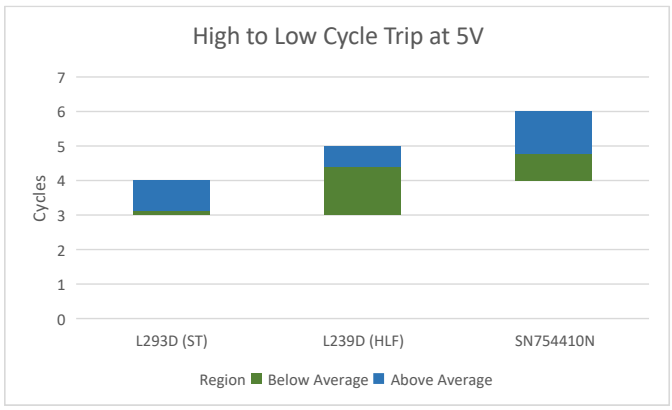


Fig. 11 High to Low cycle trip region of L293D (ST), L293D (HLF), and SN754410N

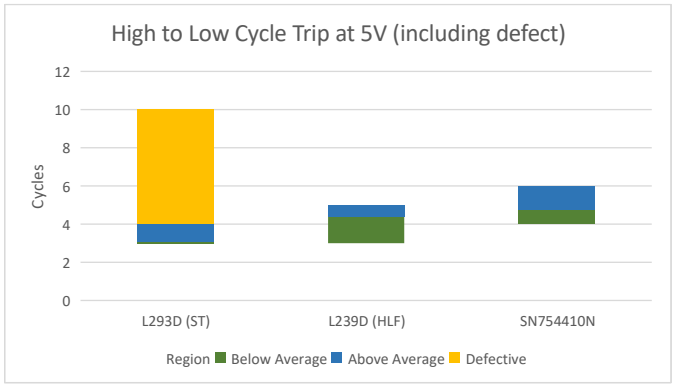


Fig. 12 High to Low cycle trip region, including the defective ICs of L293D (ST) compared to L293D (HLF) and SN754410N, shows that the cycle trip becomes longer for defective ICs

When assumed to be used in full bridge driver mode, the load performance is determined by the minimal summation of $R_{VL}$+$R_{VH}$. In test results, ST yields the minimal typical average resistance of 87.577Ω, while SN754410N gives 87.706Ω, and HLF provides 89.598Ω in the last position. The trip cycle

variants' performance, assumed to be the minimal value of $Max(C_{TH}, C_{TL})$, averages out with HLF as the fastest at 10.769 cycles, followed by SN754410N at 8.4 cycles, and ST in the last position with 12.4 cycles.

## V. Conclusion

Based on the test results, it can be concluded that the three IC variants exhibit varying delivery capabilities and switching delay times. The optimal current-carrying capability, assessed by the total virtual resistance of LOW and HIGH outputs when assumed to be operating in full bridge mode, follows a sequence. ICs from ST demonstrate the best performance, followed by SN754410N, with HLF being the least favorable. While this characteristic positions ST as more effective in regulating current to the load in electric motor applications, it is noteworthy that the switching delay for ST is the longest compared to other IC variants. Conversely, the HLF IC exhibits the shortest self-switching delay, followed by the SN754410N and ST variants.

In half-bridge or load switch applications, all ICs exhibit better performance when establishing a connection to ground compared to connecting to Vcc. Furthermore, the test batch uncovered the presence of defective ST IC samples. These defects not only reduce their current-carrying capacity but also extend the switching delay. The occurrence of defective samples within batches may be attributed to inadequate quality control measures.

## VI. Further Research Suggestions

The conducted tests and comparisons have not considered the relationship between pin positioning, conductivity, and switching delay time. Given that pin layout and production design can influence both parameters, exploring these aspects could help determine the most suitable pin driver for responsive control requirements. Additionally, it's worth noting that the research has not included comparisons involving SMD versions of ICs, such as the L293DD. Hence, it is hoped that future tests will encompass a more comprehensive analysis of these factors.

## References

[1] P. Ramya et al., "Computer Vision Controlled Automated Paint Sprayer Using Image Processing and Embedded System," Ciência & Engenharia - Science & Engineering Journal, vol. 11, no. 1, pp. 1902-1909, 2023. [Online]. Available: https://seer-ufu-br.online
[2] G. Peng, T. L. Lam, C. Hu, Y. Yao, J. Liu, and F. Yang, "Composition of Robot System," in Introduction to Intelligent Robot System Design, Springer, Singapore, 2023, doi: 10.1007/978-981-99-1814-0_1.
[3] *SN754410 Quadruple Half-H Driver*, Texas Instruments, 2015.
[4] C. Siu, "Introduction to the BJT," in Electronic Devices, Circuits, and Applications, Springer, Cham, 2022, doi: 10.1007/978-3-030-80538-8_4.
[5] M. Diallo and R. Herring, "Implementing a Battery Disconnect Switch Using 100-V Half-Bridge Gate Drivers," Texas Instruments, SLUAA58, May 2020.
[6] Allegro Microsystems, "A4957 Full Bridge MOSFET Driver," March 17, 2022, A4957-DS, Rev. 2, MCO-0000812.
[7] *L293x Quadruple Half-H Drivers*, Texas Instruments, 2016.
[8] *Push-Pull Four Channel Driver With Diodes*, ST, 2003.
[9] (2012) sn754410ne h-brige problem on PICAXE Community Forum. [Online]. Available: https://picaxeforum.co.uk/threads/sn754410ne-h-brige-problem.22629/
[10] S. F. Barrett, "Arduino II: Systems," illustrated ed. Springer International Publishing AG, 2022.
[11] Microchip Technology Inc., "ATmega48A/PA/88A/PA/168A/PA/328/P megaAVR® Data Sheet," DS40002061B, Microchip Technology Inc., 2020.